Journal of Applied Polymer Science

Oil-spill cleanup: The influence of acetylated curaua fibers on the oil-removal capability of magnetic composites

Eldho Elias,[1,2,3] Raphael Costa,[1] Fernanda Marques,[1] Geiza Oliveira,[4] Qipeng Guo,[3] Sabu Thomas,[2,5] Fernando G. Souza Jr[1]

[1]Instituto de Macromoléculas Professora Eloisa Mano, Universidade Federal do Rio de Janeiro, Rio de Janeiro 21940-310, Brazil
[2]School of Chemical Sciences, Mahatma Gandhi University, Kottayam 686560, India
[3]Institute for Frontier Materials, Deakin University, Locked Bag 2000, Geelong, Victoria 3220, Australia
[4]Departamento Química, Universidade Federal do Espírito Santo, Vitória 29060-290, Brazil
[5]International and Interuniversity Centre for Nanoscience and Nanotechnology, Mahatma Gandhi University, Kottayam 686560, India
Correspondence to: F. Marques (E-mail: fernando_gomes@ima.ufrj.br)

ABSTRACT: A magnetic resin based on cardanol, furfural, and curaua fibers was prepared and characterized. The material could be used in oil-spill cleanup processes, because of its aromatic/aliphatic balance. The resin was prepared through bulk polycondensation of cardanol and furfural in the presence of curaua fibers and maghemite nanoparticles. Hydrophobicity of the curaua fibers was improved by acetylation, increasing the oil-absorbing capability of the composites. The obtained magnetic composites were studied by Fourier-transform infrared spectroscopy, X-ray diffraction, and thermogravimetric analysis. Degree of cure, magnetic force, and oil-removal capability tests were also performed. The results show that the composites possess an elevated cure degree in addition to a considerable magnetic force. The materials exhibit a good oil removal capability in the presence of a magnetic field, which is improved by the use of acetylated curaua. In the best case, the composite filled with maghemite and curaua can remove 12 parts of oil from water. © 2014 Wiley Periodicals, Inc. J. Appl. Polym. Sci. **2015**, *132*, 41732.

KEYWORDS: biopolymers and renewable polymers; composites; thermosets

Received 26 June 2014; accepted 6 November 2014
DOI: 10.1002/app.41732

INTRODUCTION

Although petroleum is the most important energy[1] and raw material source for various synthetic chemicals,[2] its use always involves a considerable risk of oil spillage[3,4] that could occur during its transportation and storage.[5] Oil spills in land, river, or ocean environments impose a major threat on the environment, because they have a severe impact on the environment,[6–10] marine life, and industries such as the food and tourism trades.[11–15]

Nowadays, the techniques used up for oil-spill cleanup can be categorized as mechanical, chemical,[16] or bioremediation methods.[8] The mechanical method uses booms[17] to reduce the spreading of the oil, while skimmers[10] are used to recover the oil from the surface of the water.[16] The use of chemical dispersants[18] and surfactants[19] are normal among the available chemical methods for oil-spill cleanup. Spraying of dispersants helps to break up oil slicks into smaller droplets and solidifiers react with the oil to form cohesive, solidified masses that floats on water.[14] The third method, bioremediation, uses living organisms to remove pollutants from the environment[20,21] and should always be considered.

The devastation extension caused by accidents, such as that in Dalian/China (2010), in the Gulf of Mexico (2010), in Campos/Brazil (2011), as well as in Arkansas/USA (2013), shows that new strategies for remediation must be continuously studied.[12,22] The oil-cleanup process will be more effective if the sorbent material presents biodegradability, uptake capability, hydrophobicity, reusability, and cost effectiveness. In this context, our group focuses on the use of renewable resources that can be transformed into polymeric materials with good biodegradability as well as oil absorptivity for oil-spill cleanup applications.[11–15]

Among the available renewable resources, cashew nutshell liquid (CNSL), which is an inexpensive byproduct of the cashew industry, is very promising. The main component of CNSL is cardanol, a phenol derivative with a C15 unsaturated

Table I. Characteristics of the Oil Used for OR Analysis

Oil	Density (g cm^{-3})	^{0}API (60°F)[a]	Viscosity (mPa s)
1	0.9726	13.41	7006
2	0.9279	20.36	348

[a] The American Petroleum Institute gravity.

hydrocarbon at its *meta*-position.[23,24] Cardanol can be obtained from CSNL by distillation, and its phenolic resins present oil absorption properties, owing to their aliphatic/aromatic character.[12,15,22] Going further into the use of renewable resources in environmental recovery, natural fibers, such as cotton, bark, kenaf, vegetable fibers, rice husk, and wool are extensively studied as materials for the oil-spill cleanup process.[25–30] Lignocellulosic fibers mainly consist of three important components, that is, cellulose, lignin, and hemicelluolose. This complex fiber structure can help to tune the aliphatic/aromatic nature of polymeric composites when dispersed into the polymeric matrix. Among these cellulosic biomasses, curaua fibers are a potential agricultural waste mass, which is cultivated in the Amazon region of Brazil.[31]

In addition, the oil-spill cleanup process can be improved by the use of magnetic particles, which absorb contaminants from aqueous or gaseous effluents and, after sorption, can be separated from the medium by a simple magnetic process.[32] The use of magnetic nanoparticles such as maghemite in association with biopolymers may improve oil-sorption characteristics and, thus, provide a new class of composite materials that are able to absorb petroleum from water.

The main objective of this work involves the investigation of curaua fibers and their effect on the oil absorption capability of the cardanol–furfural resin. To improve the polymer–fiber adhesion and to reduce water absorption, the surfaces of the curaua fibers were chemically modified by acetylation. The produced materials were characterized using Fourier-transform infrared spectroscopy (FTIR), X ray diffraction (XRD), and thermogravimetric analysis (TGA). In addition, the magnetic force, oil-removal (OR) capability, and reusability of the sorbents were investigated. The results show that the composites possess an elevated cure degree in addition to a considerable magnetic force. The materials exhibit a good OR capability in the presence of a magnetic field, which is improved by the use of acetylated curaua. In the best case, the composite filled with maghemite and curaua can remove 12 parts of oil from water.

EXPERIMENTAL

Materials

Cardanol was kindly supplied by Companhia Brasileira de Resinas—RESIBRAS. Furfural, sulfuric acid, ferric chloride ($FeCl_3$), anhydrous sodium sulfite (Na_2SO_3), acetic anhydride, and sodium hydroxide (NaOH) were purchased from Vetec/Brazil at analytical grade. Hydrochloric acid (HCl) was purchased from Proquímica/Brazil at analytical grade. All of these reagents were used as received. Two different types of oils were used in order to check the oil-absorption analysis. The characteristics of the investigated oils are presented in Table I.

Methods

Maghemite Particle Synthesis. The syntheses of the maghemite particles were performed as described in previously published reports.[12,14,15,33–35] Initially, aqueous solutions of HCl (2*M*), $FeCl_3$ (2*M*), and sodium sulfite (1*M*) were prepared. In a typical procedure, 30 mL of the $FeCl_3$ solution and 30 mL of deionized water were added to a beaker under continuous agitation. Soon afterwards, 20 mL of the sodium sulfite solution was added to the beaker, also under continuous agitation. The reaction product was precipitated by slowly adding 51 mL of concentrated ammonium hydroxide into the beaker under continuous agitation. After 30 min, the medium was filtered and the obtained particles were washed several times with water before they were finally dried at 80°C in an oven. Magnetite was converted into maghemite by annealing at 250°C for 1 h.

Acetylation of Curaua Fibers. Acetylation of curaua fibers was performed with acetic anhydride (100 mL) and concentrated sulfuric acid (0.25 mL) as a catalyst in a three-necked round-bottomed flask equipped with a reflux condenser.[30,36] The flask was placed in an oil bath, which was set at the required temperature (80°C) using atmospheric pressure, with a reflux condenser fitted. After the reaction had proceeded for the required time (1 h), the flask was removed from the oil bath and the hot reagent was decanted. Resultant curaua fibers were then purified by washing with acetone and ethanol in order to eliminate reaction byproducts. Finally, the acetylated curaua fibers were oven-dried under vacuum at 60°C for 12 h. The dried fibers were weighed in order to determine the increase in weight compared to the initial weight. To confirm the acetylation, the percentage increase of the mass (PIM) of the curaua fibers were calculated using the formula shown in Eq. 1:

$$\mathrm{PIM} = 100 \times \frac{W_2 - W_1}{W_1} \tag{1}$$

in which W_I and W_2 are the weights of the curaua fibers and acetylated curaua fibers, respectively.

Resin Synthesis and Preparation of the Composite. Cardanol–furfural resin was prepared through acid catalysis. 45 g of cardanol was mixed with 36 g of furfural in a three necked flask (250 mL) for 2 h under continuous stirring at room temperature. Then the solution was heated up to 75°C and few drops of sulfuric acid were added as acid catalyst. Stirring was maintained until the formation of a solid material. The solid material was recovered from the three necked flask and dried in an air oven at 100°C overnight. All the obtained materials were submitted to density and oil removal capability tests. The experimental procedure for preparing resins with magnetic properties was similar to the one described for the resin preparation. In these cases, to assure complete dispersion of the magnetic filler as well as the curaua fibers in the reaction medium, maghemite, and curaua fibers were inserted before acidification. Magnetic composites were prepared using 1, 5, and 9 wt % of maghemite with respect to the amount of cardanol used up for the reaction. They were named MC1, MC5, and MC9, respectively. Magnetic nanocomposites containing 9 wt % maghemite were also prepared using 1, 5, and 9 wt % of curaua fibers (here also, amount of curaua fiber was taken with respect to the amount

of cardanol used up for the reaction). These composites were named MC9F1, MC9F5, and MC9F9, respectively.

Characterization

FTIR spectra were collected with a Varian 3100 FTIR (Excalibur series) using an attenuated total accessory reflectance mode. The resolution was equal to 4 cm^{-1} and accumulation was performed for 24 scans.

TGA of the pure resin and the composite resins was performed using a Shimadzu TGA instrument. The samples were heated from 25 to 800°C using a heating rate equal to 10°C min^{-1} with a nitrogen flow of 100 mL min^{-1}.

The surface morphologies of the raw fibers and the acetylated curaua fibers were analyzed using a scanning electron microscope (JEOL JSM-5610 LV). Specimens were carefully prepared and coated with a thin layer of gold metal to assist image formation.

XRD tests were performed using a Rigaku Miniflex X ray diffractometer in a 2θ range from 2° to 80° using the FT (fixed time) method. Programmed steps, equal to 0.05° per second, were performed using a tube voltage and current equal to 30 kV and 15 mA, respectively. The radiation used was CuKα, equal to 0.1542 nm.

The direct estimation of cellulose, hemicellulose, and lignin present in the raw and modified fibers followed the procedure described by Moubasher.[37] In a typical procedure, a known amount of curaua fiber (2 g) was washed in ethanol and dried in an oven at 40°C overnight. The obtained material was divided into two equal parts. One part was considered as fraction A. The second part was treated with a KOH solution (24%) for 4 h at 30°C, and soon afterwards the medium was filtered, the residue was washed with distilled water, and then dried at 80°C overnight; the dry weight was taken as fraction B. The same sample was treated with 72% H_2SO_4 for 3 h. The obtained medium was filtered and H_2SO_4 was removed by washing with distilled water and drying at 80°C in an oven overnight; the dry weight was taken as fraction C. The difference in weight between fractions A and B corresponded to the total hemicellulose content in the curaua fibers. Fraction C was considered to be the lignin content of the fibers, whereas the weight difference between fractions B and C was calculated as the cellulose content inside the fibers.

The density of resin and composite materials was determined in triplicate at 20°C, using a picnometer. Degree of cure was monitored by means of a Soxhlet extractor for 72 h, using cyclohexane/toluene (1:1 by volume) as the solvent. In addition, flotation capability tests were performed in water and in ethanol. In each case, 1 g of the resin was poured on to the liquid surface. After 5 min, a visual inspection was performed and qualitative results were registered.[12]

The magnetic force was determined using a test fully described elsewhere.[38] This setup constituted a Shimadzu AY-220 analytical balance, an ICEL PS-4100 voltage source, an ICEL MD-6450 digital multimeter, a TLMP-Hall-02 Gaussmeter GlobalMag, a custom-built sample holder, and an electromagnet. System

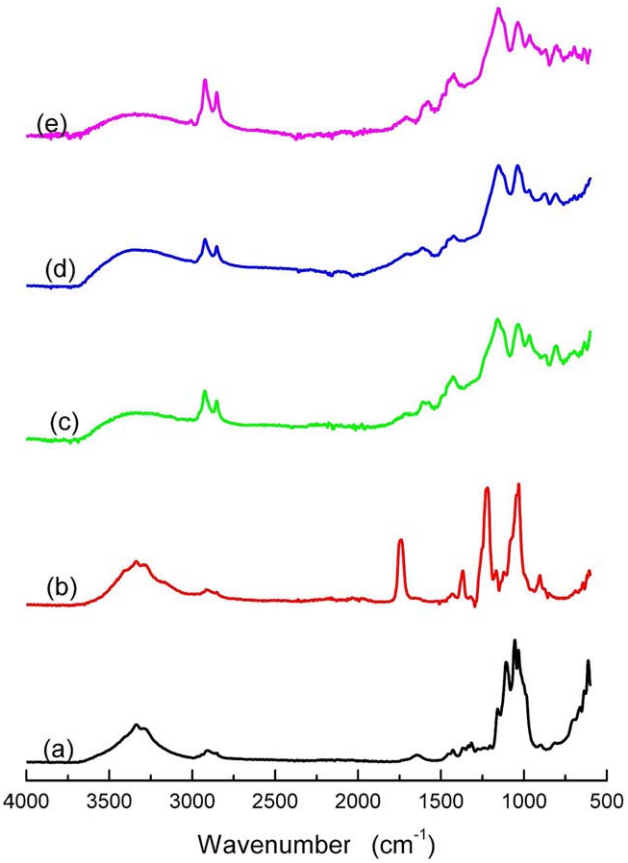

Figure 1. FTIR spectra of the raw curaua fiber (a), acetylated curaua (b), pure resin (c), and magnetic composites containing with 5 wt % (d), and 9 wt % (e) acetylated curaua fiber. [Color figure can be viewed in the online issue, which is available at wileyonlinelibrary.com.]

calibration was performed in the absence of magnetic material. Firstly, using the ampere meter and the Gaussmeter, a current versus magnetic field calibration was performed. Soon afterwards, a current versus mass calibration was also performed. The obtained results were used to predict part of the presented error. Magnetic force tests were performed following mass variation in the sample in the presence of different magnetic fields produced by the electromagnet. Then, the apparent variation in the mass of the sample in the presence of magnetic field was calculated by subtracting the mass of the sample in presence of magnetic field from the initial mass of sample. The magnetic force (opposite to the gravitational force) was calculated according to eq. 2:

$$F_m = \Delta m \times g \quad (2)$$

in which F_m is the magnetic force, Δm is the apparent variation in the mass in the presence of the magnetic field, and g is the acceleration of gravity. As a reference, the magnetic force of a standard cobalt(II) chloride hexahydride sample was calculated according to this method, and the obtained result was equal to 0.19 ± 0.02 mN at 840 ± 2 Gauss.

The oil removal (OR) capability tests were performed according to the analytical procedure established in our laboratory.[12,22,39] Gravimetric OR capability was evaluated in the following way.

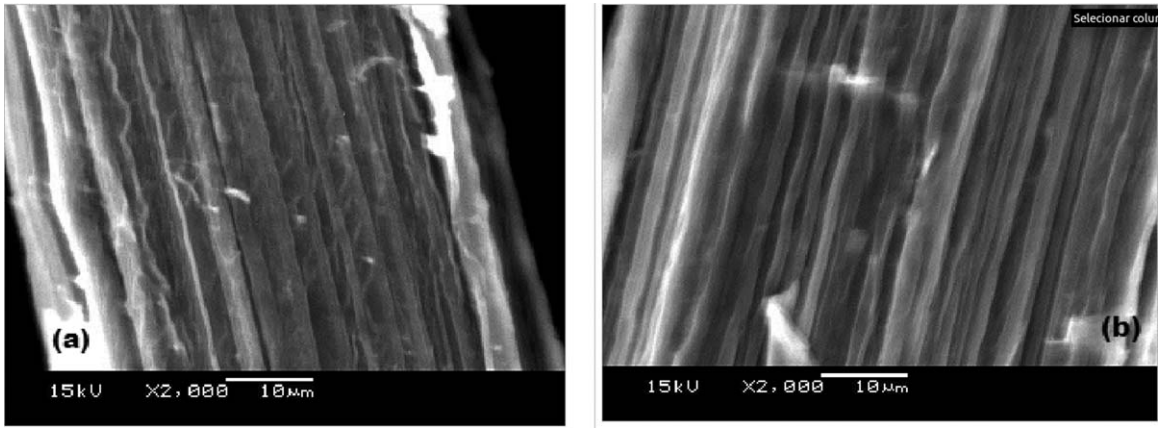

Figure 2. SEM images of the raw (a) and acetylated (b) curaua fibers.

Firstly, the magnetic composite was weighed (m_1), then 90 mL water was poured into a beaker and the total mass was determined. Secondly, a known mass of the oil (m_2) was spilt on the water and the magnetic composite was added into the beaker containing the water, and the oil. After 5 min, the oil and the composite were magnetically removed. Finally, the mass of the oil residue could be determined (m_3) and the gravimetric OR was calculated according to eq. 3:

$$\mathrm{OR} = \frac{m_2 - m_3}{m_1} \quad (3)$$

Weighing was carried out with the help of an analytical scale.

In order to examine the reusability of the sorbents, the mixture containing both the oil and the resin, after oil recovery, was transferred to a beaker containing 25 mL toluene. After strong agitation, the sorbent was separated from the oil through a filtration method. The resin was dried and weighed. The dried resin was used again in the oil-recovery process, as before, in order to examine the reusability of the sorbent.

RESULTS AND DISCUSSION

Fibers were characterized by FTIR analysis, which provided the main differences between the untreated and treated materials. Figure 1 presents the obtained FTIR spectra of the different fibers and composite materials.

One of the characteristic bands presented in the FTIR spectrum of the fiber is a wide band around 3338 cm^{-1}, which is assigned to the stretching of OH. This band is wide, because the OH group is able to make hydrogen bonds. The doublet at 2910 and 2856 cm^{-1} is assigned to C—H stretching. The characteristic band at 1746 cm^{-1} is attributed to C═O ester stretching, whereas the characteristic band at 1640 cm^{-1} is referenced to conjugated C═O aldehyde and C═C stretching.

The characteristic band at 1433 cm^{-1} corresponds to the C—C stretching of an aromatic ring (aromatic skeleton vibration). Besides, this band can be attributed to O—H scissoring deformation in the plane of the ring together with the band at 1321 cm^{-1}. The C—H stretching can be seen at 1374 cm^{-1}. The characteristic band at 1226 cm^{-1} is ascribed to C═O aromatic stretching. The band at 1179 cm^{-1} corresponds to C—O—C asymmetric stretching, and symmetric stretching of this bond appears at 1114 and 1173 cm^{-1}. The characteristic band at 1161 cm^{-1} is O—C—C stretching together with the band at 1032 cm^{-1}. Therefore, the band at 1032 cm^{-1} represents conjugated C—O—C and O—C—C. The bands observed at 895 and 653 cm^{-1} are characteristic of C—H scissoring deformation in the aromatic ring.[31]

FTIR results [Figure 1(a,b)] provide evidence for the surface modification of curaua fibers through acetylation. The characteristic band at 1735 cm^{-1} in the modified curaua fiber spectrum indicates the presence of an ester group. The reduction of the intermolecular hydrogen bonding between 3300 and 3400 cm^{-1} confirms the introduction of the acetyl groups in the curaua fibers, thus replacing the hydroxyl groups. These results are in agreement with previously published data related to the acetylation of natural fibers.[40,41]

The FTIR spectrum of the pure resin [Figure 1(c)] presented a wide band around 3425 cm^{-1}, which can be attributed to the stretching of OH that can produce hydrogen bonding. The band at 3008 cm^{-1} corresponds to the stretching of CH, and the doublet at 2923 and 2852 cm^{-1} is ascribed to the stretching of CH_2 and CH_3, respectively. The characteristic band at 1586 cm^{-1} indicates aliphatic C═C stretching, whereas the stretching of the aromatic double bonds (C═C) takes place at 1483 and 1453 cm^{-1}. C—O stretching of the phenol group can be observed at 1159 and 1036 cm^{-1}. The characteristic band at 966 cm^{-1} corresponds to the C═C asymmetric stretching of the aromatic ring, whereas the bands at 876 and 715 cm^{-1} are the characteristic scissoring deformation of ring out-of-plane hydrogen. The O—H scissoring deformation appears at 601 cm^{-1}.

These results indicate that the obtained resins are typical phenol–furfural resins and that the polymerization occurred through aromatic rings.[11] In turn, the composite spectra reflect the composition of the ingredients (resin, acetylated fiber) ingredients.

SEM images of raw and acetylated curaua fibers are shown in Figure 2.

From Figure 2(a), the surface of the raw curaua fiber is observed to be covered by a waxy layer, which leads to the

Table II. Composition of Raw and Acetylated Curaua Fibers

Fiber	Cellulose (%)	Hemicellulose (%)	Lignin (%)
Raw	69.6 ± 0.7	18.6 ± 0.6	9.4 ± 0.2
Acetylated	63.2 ± 0.5	20.5 ± 0.7	10.3 ± 0.4

rough morphology observed.[42,43] In addition, the thickness of the waxy layer is not uniform. However, Figure 2(b) shows a smoother surface for the acetylated curaua fibers in comparison with the rough surface of the raw fiber, which can be attributed to removal of the waxy substance during the acetylation reaction.

The degree of acetylation was estimated using the PIM method. After acetylation, the modified fibers should present a weight increase in comparison with raw ones.[30,44] Experimental results are in agreement with previously published reports, and the calculated degree of acetylation was 10.3 ± 0.5%, which confirmed surface modification through acetylation. In addition, the effect of acetylation on the final composition of the fibers was studied and the results are shown in Table II.

Results from Table II show that the overall percentage of cellulose inside the curaua fibers was reduced during acetylation. However, the amount of hemicellulose and lignin remained almost unaffected, as reported elsewhere by Tserki's group.[43] During acetylation, large acetyl groups replace the comparatively small hydroxyl groups, leading to a decrease in the hydrogen-bonding force and an increase in the hydrophobicity, which may be very useful in the oil-cleanup processes. This assumption was proven by a sorption test. Raw and acetylated fibers were able to absorb 2.72 ± 0.43 and 1.24 ± 0.36 g of water, respectively.

Figure 3 shows the XRD patterns of the studied materials. Pure resin showed an amorphous halo [Figure 3(a)], whereas maghemite [Figure 3(e)] showed crystalline peaks at $2\theta = 30.7°$, 36.2°, 43.6°, 57.7°, and 63.2°. These crystalline peaks correspond to

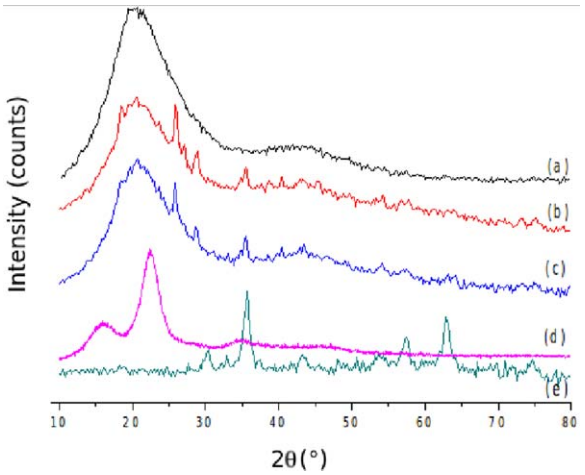

Figure 3. XRD patterns of the pure resin (a), composites MC9F5 (b) and MC9F9 (c), acetylated curaua fiber (d), and maghemite (e). [Color figure can be viewed in the online issue, which is available at wileyonlinelibrary.com.]

Table III. Crystal Size and Crystallinity Degree of the Analyzed Materials

Samples	Crystal size (nm)	Crystallinity degree (%)
Resin	–	23 ± 1
MC9	11 ± 1	37 ± 2
MC9F5	10 ± 2	23 ± 2
MC9F9	11 ± 1	27 ± 2
Maghemite	10 ± 2	78 ± 1

the (2 2 0), (3 1 1), (4 0 0), (5 1 1), and (4 4 0) reflections, respectively, of a spinel crystal structure, such as that presented by maghemite.[45–47] In addition, the crystallinity degree was calculated according Ruland's method and crystal sizes were calculated using Scherer's equation (eq. 4), with the peak corresponding to the (3 1 1) crystal plane.

$$CS = \frac{k.\lambda}{\Delta\theta.\cos(\theta)} \quad (4)$$

In eq. 4, CS is the crystal size, k is a constant (equal to 1.0), λ is the wavelength, θ is the Bragg angle, and $\Delta\theta$ is the full width at half maximum (FWHM) of the (3 1 1) peaks.

As shown in Table III, maghemite presented a crystallinity degree and a crystal size equal to 78 ± 1% and 10 ± 2 nm, respectively.

All of the magnetic composites presented maghemite particles with the same crystal size. The average value obtained was 11 ± 1 nm, indicating that the crystalline structure of the magnetic filler inside the composites was statistically equal. In turn, as shown in Table III, composites filled with maghemite (MC9) nanoparticles showed a higher degree of crystallinity compared to that of the pure resin. However, composites containing acetylated fibers along with maghemite nanoparticles presented a crystallinity degree similar to that of the pure resin. This result is interesting, because the incorporation of curaua fibers decreases the total crystallinity of the composites, thereby lowering the density of the materials, allowing them to float easily on water.

Density, degree of cure and flotation capability of the neat resin as well as composites was analyzed and the obtained results are shown in Table IV. The flotation capability tests allowed us to infer that the composites are able to float on water, but that they sink in ethanol. In addition, previous observations are supported by the density results (Table IV), which range from 0.84 to 0.92 g cm^{-3}. Therefore, the obtained density results indicate that the composites can act as good oil-absorbing materials, because they are able to float on the contaminated water.

The calculated degree of curing values of the composites is also shown in Table IV. All composites presented have a cure degree in the range 90–94%. These high degree of curing values indicate that the composites are insoluble in common organic solvents, meaning that petroleum can be recovered from the composites.

As shown in Figure 4, the prepared materials were also studied using TGA thermograms.

Table IV. Floatability, Density, and Cure Degree of the Resin and Composites

Sample	Maghemite (%vol)	Curaua (%vol)	Floatability		Density (g cm^{-3})	Degree of cure (%)
			Water	Ethanol		
Resin	–	–	+	–	0.84 ± 0.12	90 ± 2
MC9	5.0	–	+	–	0.87 ± 0.11	94 ± 1
MC9F5	5.0	2.5	+	–	0.92 ± 0.19	93 ± 1
MC9F9	5.0	5.0	+	–	0.89 ± 0.24	91 ± 3

The initial weight loss at 75°C was considered to be water loss in the form of moisture absorption. The second stage of degradation (onset at 230°C) is related to the decomposition of hemicellulose.[48,49]

The final stage of degradation begins at 286°C, and the maximum decomposition rate presented at 349°C. This last value is attributed to the degradation of the cellulose fraction in the curaua fibers. Thermogravimetric analysis of the raw and acetylated curaua fibers indicated that, in the initial stage of the degradation (at 250°C), the raw fibers and the acetylated fibers lost 4.5 and 10.7% of their initial weight, respectively. Therefore, these results indicate that curaua fibers show higher thermal stability in comparison with the acetylated fibers, possibly due to the degradation of part of the macromolecules during acetylation.

Thermogravimetric analysis of the composites indicate that the curaua reinforced composites are more thermally stable than the pure resin (Figure 4). The TGA thermograms of the resin and composite samples showed that an initial weight loss at 70–80°C could be attributed to the elimination of water adsorbed in the materials.[50]

The TGA thermograms of the resins showed inflections at 340 and 400°C, which are attributed to the thermal degradation of the curaua and thermoset resins, respectively. Table V clearly indicates the increase in the onset temperature of the composites as higher amounts of the fiber are used.

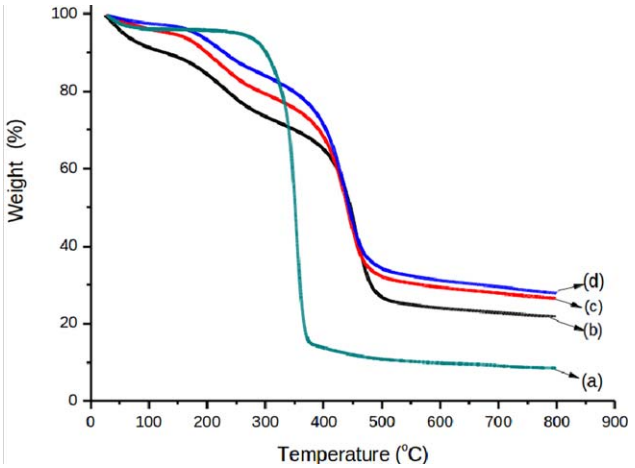

Figure 4. TGA thermograms of curaua fiber (a), pure resin (b), composite filled with 5 wt % (c), and 9 wt % of the acetylated fiber (d). [Color figure can be viewed in the online issue, which is available at wileyonlinelibrary.com.]

From the thermogravimetric analysis, it can be seen that the weight loss of the composites (MC9F5 and MC9F9) was found to be lower than the that of the pure resin up to 340°C, which means that the degradation of the composite was delayed in comparison with the pure resin. From Table V, it can be seen that there was no significant difference for weight loss that occurred for the composites and the resins beyond 400°C, as the curaua content of the analyzed materials had completely degraded.

The magnetic force of the materials was studied. The synthesized maghemite nanoparticles presented a magnetic force (at 800 G) equal to 958.0 ± 0.4 mN. In turn, composites containing 1, 5, and 9 wt % of maghemite presented magnetic forces (at 800 G) equal to 4.7 ± 0.4, 8.9 ± 0.6, and 23.0 ± 0.8 mN, respectively.

Among the prepared magnetic composites, the one possessing 9 wt % maghemite (MC9) was selected as the optimized material for oil removal tests, because of its higher magnetic force as well as its good dispersion inside the resin. The curaua–fiber-incorporated magnetic composites were then prepared by the addition of 1, 5, and 9 wt % of the fibers into the composite using the optimized magnetic force (MC9). The obtained materials, containing different amounts of acetylated curaua fibers, were used in the oil removal tests. The results related to the

Table V. Thermal Analysis of the Resin and Composites

Sample	Onset (°C)	Weight loss (%)	
		@ 340°C	@ 400°C
Resin	55	25	40
MC9F5	145	23	39
MC9F9	182	19	38

Table VI. Magnetic Force Analysis and OR Capabilities of the Analyzed Materials

Sample	Magnetic force (mN)	OR capability (g g^{-1})	
		Oil 1	Oil 2
MC9	23.0 ± 0.8	10.25 ± 0.35	2.03 ± 0.05
MC9F1	23.0 ± 0.2	10.93 ± 0.24	2.35 ± 0.55
MC9F5	21.3 ± 0.6	12.65 ± 0.21	2.78 ± 0.75
MC9F9	20.9 ± 0.4	12.38 ± 0.18	2.85 ± 0.50

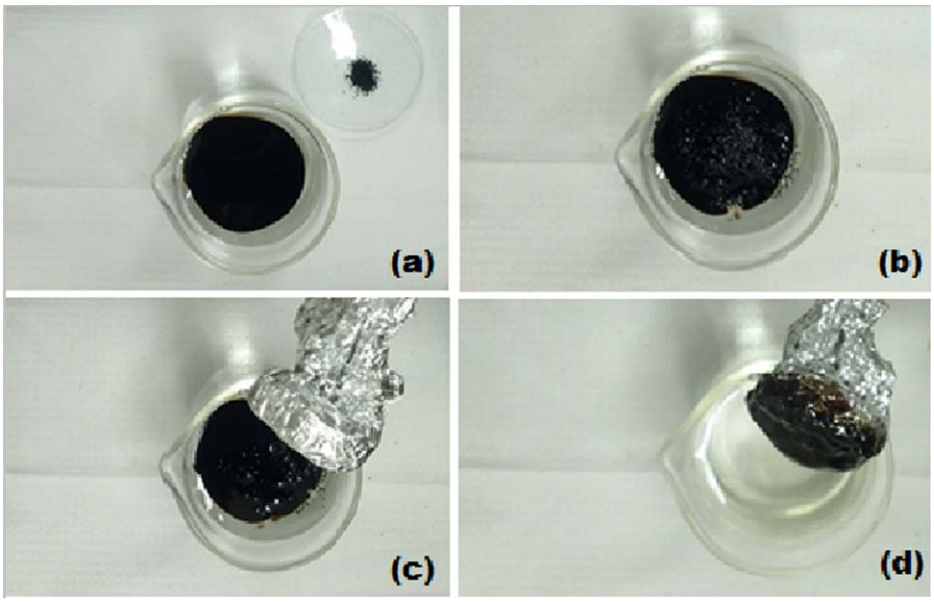

Figure 5. Oil-spill cleanup process using magnetic composites. Oil spill on the water and magnetic composite (a), insertion of the composite on the surface of oil spill (b), magnet close to mixture (c), and the final cleanup (d). [Color figure can be viewed in the online issue, which is available at wileyonlinelibrary.com.]

magnetic force and oil removal capabilities of these composites are shown in Table VI.

Magnetic force analysis (Table VI) of the composites shows that the addition of curaua fibers to the composite leads to a slight decrease in the magnetic force of the materials, which can be attributed to the decreased fraction of magnetic nanoparticles compared to the increased organic phase. However, the oil removal capability tests show that the composites that contain higher amounts of the acetylated curaua fibers were more efficient in the cleanup process than the composites without the fibers. In addition, the oil removal tests, exemplified in Figure 5, were carried out with two types of oil that had different viscosities.

From the oil removal tests, it can be seen that all resin compositions could absorb at least 10 g of petroleum per gram of the resin from the water. The resin without fibers could absorb 10.25 ± 0.35 g g^{-1} oil, whereas composites MC9F1, MC9F5, and MC9F9 were able to sorb $10.93 \pm .24$, 12.65 ± 0.21, and 12.38 ± 0.18 g g^{-1} of Oil 1, respectively. Despite being less efficient, the same behavior was verified in the case of the low-viscosity petroleum cleanup. Table VI also makes clear that, even with the incorporation of the fibers, the composite could absorb at least 2.0 g of Oil 2 per gram of the resin from the water. Therefore, the presented materials are more appropriate to cleanup processes involving heavy oils.

After the oil removal tests, gravimetric experiments have shown that 90% of the sorbent was recovered from the oil using a filtering process. The recovered material could be reused in further cleanup experiments. Tests were performed using the MC9F5 material. In the first, second, and third reuse cycles, MC9F5 removed 12.65 ± 0.21, 11.25 ± 0.56, and 10.80 ± 0.54 g g^{-1} of Oil 1 from the water, respectively. Therefore, we can conclude that the sorbent can be reused in oil-spill cleanup applications.

CONCLUSIONS

Surface modification of curaua fibers was performed successfully using the acetylation method to make them more hydrophobic, rendering them useful for oil-absorption applications. Maghemite nanoparticles and acetylated curaua fibers were incorporated into the cardanol–furfural resin in order to prepare magnetic polymer nanocomposites. Oil removal tests showed that the resins incorporating curaua fibers could absorb 25% more oil than the neat resin, which clearly depicts the importance of the curaua fiber as a substrate for oil removal applications. The successful reuse of these materials without any significant decrease in oil removal capability makes them a potential candidate for oil recovery.

ACKNOWLEDGMENTS

The authors would like to thank to Conselho Nacional de Desenvolvimento Científico e Tecnológico—CNPq, Coordenação de Aperfeiçoamento de Pessoal de Nível Superior—CAPES, and CAPES-Nanobiotec, Financiadora de Estudos e Projetos—FINEP (ref.1889/10), and Fundação de Amparo à Pesquisa do Estado do Rio de Janeiro—FAPERJ for financial support, and for scholarships.

REFERENCES

1. Chanis, J. *Am. Foreign Policy Interest* **2012**, *34*, 20.

2. Al-Sabagh, A. M.; Kandile, N. G.; Noor El-Din, M. R. *Sep. Sci. Technol.* **2011**, *46*, 1144.

3. Peng, L.; Yuan, S.; Yan, G.; Yu, P.; Luo, Y. *J. Appl. Polym. Sci.* **2014**, *131*, 40886.
4. Li, H.; Wu, W.; Bubakir, M. M.; Chen, H.; Zhong, X.; Liu, Z.; Ding, Y.; Yang, W. *J. Appl. Polym. Sci.* **2014**, 131.
5. Annunciado, T. R.; Sydenstricker, T. H. D.; Amico, S. C. *Mar. Pollut. Bull.* **2005**, *50*, 1340.
6. Angelim, A. L.; Costa, S. P.; Farias, B. C. S.; Aquino, L. F.; Melo, V. M. M. *J. Environ. Manage.* **2013**, *127*, 10.
7. Al-Majed, A. A.; Adebayo, A. R.; Hossain, M. E. *J. Environ. Manage.* **2012**, *113*, 213.
8. Chagas-Spinelli, A. C. O.; Kato, M. T.; de Lima, E. S.; Gavazza, S. *J. Environ. Manage.* **2012**, *113*, 510.
9. Mendoza-Cantú, A.; Heydrich, S. C.; Cervantes, I. S.; Orozco, O. O. *J. Environ. Manage.* **2011**, *92*, 1706.
10. Vandermeulen, J. H.; Ross, C. W. *J. Environ. Manage.* **1995**, *44*, 297.
11. Ferreira, L. P.; Moreira, A. N.; Delazare, T.; Oliveira, G. E.; Souza, Jr. F. G. *Macromol. Symp.* **2012**, *319*, 210.
12. Grance, E. G. O.; Souza, Jr. F. G.; Varela, A.; Pereira, E. D.; Oliveira, G. E.; Rodrigues, C. H. M. *J. Appl. Polym. Sci.* **2012**, *126*, 305.
13. Lopes, M. C.; Souza, Jr. F. G.; Oliveira, G. E. *Polímeros* **2010**, *20*, 359.
14. Oliveira, G. E.; Souza, Jr. F. G.; Lopes, M. C. In Natural Polymers, Biopolymers, Biomaterials, and Their Composites, Blends, and IPNs; CRC Press Book: NJ, **2012**; Chapter 23, p 370.
15. Souza, Jr. F. G.; Oliveira, G. E.; Lopes, M. C. In Natural Polymers, Biopolymers, Biomaterials, and Their Composites, Blends, and IPNs; CRC Press Book: NJ, **2012**; Chapater 22, p 359.
16. Nordvik, A. B. *Spill Sci. Technol. Bull.* **1999**, *5*, 309.
17. El-Fadel, M.; Abdallah, R.; Rachid, G. *J. Environ. Manage.* **2012**, *113*, 93.
18. Gong, Y.; Zhao, X.; O'Reilly, S. E.; Qian, T.; Zhao, D. *Environ. Pollut.* **2014**, *185*, 240.
19. Boonyasuwat, S.; Chavadej, S.; Malakul, P.; Scamehorn, J. F. *Sep. Sci. Technol.* **2009**, *44*, 1544.
20. Sarkar, D.; Ferguson, M.; Datta, R.; Birnbaum, S. *Environ. Pollut.* **2005**, *136*, 187.
21. Bragg, J. R.; Prince, R. C.; Harner, E. J.; Atlas, R. M. *Nature* **1994**, *368*, 413.
22. Souza, Jr. F. G.; Marins, J. A.; Rodrigues, C. H. M.; Pinto, J. C. *Macromol. Mater. Eng.* **2010**, *295*, 942.
23. Huong, N. L.; Nieu, N. H.; Tan, T. T. M.; Griesser, U. J. *Angew. Makromol. Chem.* **1996**, *243*, 77.
24. Besteti, M. D.; Cunha, A. G.; Freire, D. M. G.; Pinto, J. C. *Macromol. Mater. Eng.* **2014**, *299*, 135.
25. Dhakal, H. N.; Zhang, Z. Y.; Richardson, M. O. W. *Compos. Sci. Technol.* **2007**, *67*, 1674.
26. Joffe, R.; Andersons, J.; Wallström, L. *Compos. Part Appl. Sci. Manuf.* **2003**, *34*, 603.
27. Ouajai, S.; Shanks, R. A. *Polym. Degrad. Stab.* **2005**, *89*, 327.
28. Rao, K. M. M.; Rao, K. M. *Compos. Struct.* **2007**, *77*, 288.
29. Shi, J.; Shi, S. Q.; Barnes, H. M.; Horstemeyer, M.; Wang, J.; Hassan, E.-B. M. *Int. J. Polym. Sci.* **2011**, *2011*, 1.
30. Teli, M. D.; Valia, S. P. *Carbohydr. Polym.* **2013**, *92*, 328.
31. Souza, Jr. F. G.; Oliveira, G. E.; Rodrigues, C. M.; Soares, B. G.; Nele, M.; Pinto, J. C. *Macromol. Mater. Eng.* **2009**, *294*, 484.
32. Nassar, N. N. *Sep. Sci. Technol.* **2010**, *45*, 1092.
33. Costa, R. C. da; Souza, Jr. F. G. *Polímeros Ciênc. E Tecnol.* **2014**, *24*, 243.
34. Pereira, E. D.; Souza, Jr. F. G.; Soares, D. Q. P.; Santana, C. I.; Lemos, A.; Menezes, L. *Polym. Eng. Sci.* **2013**.
35. Souza, Jr. F. G.; Marins, J.; Pinto, J.; de Oliveira, G.; Rodrigues, C.; Lima, L. *J. Mater. Sci.* **2010**, *45*, 5012.
36. Li, X.; Tabil, L. G.; Panigrahi, S. *J. Polym. Environ.* **2007**, *15*, 25.
37. Moubashe, M.; Abdel-Hafez, S.; Abdel-Fattah, H.; Mohanram, A. *J. Agric. Res.* **1982**, *46*, 1467.
38. Souza, Jr. F. G.; Ferreira, A. C.; Varela, A.; Oliveira, G. E.; Machado, F.; Pereira, E. D.; Fernandes, E.; Pinto, J. C.; Nele, M. *Polym. Test.* **2013**, *32*, 1466.
39. Varela, A.; Oliveira, G.; Souza, F. G.; Rodrigues, C. H. M.; Costa, M. A. S. *Polym. Eng. Sci.* **2013**, *53*, 44.
40. Johar, N.; Ahmad, I.; Dufresne, A. *Ind. Crops Prod.* **2012**, *37*, 93.
41. Lin, N.; Huang, J.; Chang, P. R.; Feng, J.; Yu, J. *Carbohydr. Polym.* **2011**, *83*, 1834.
42. Sreekala, M. S.; Kumaran, M. G.; Thomas, S. *J. Appl. Polym. Sci.* **1997**, *66*, 821.
43. Tserki, V.; Zafeiropoulos, N. E.; Simon, F.; Panayiotou, C. *Compos. Part Appl. Sci. Manuf.* **2005**, *36*, 1110.
44. Adebajo, M. O.; Frost, R. L. *Spectrochim. Acta A: Mol. Biomol. Spectrosc.* **2004**, *60*, 2315.
45. Govindaraj, B.; Sastry, N. V.; Venkataraman, A. *J. Appl. Polym. Sci.* **2004**, *93*, 778.
46. Hyeon, T.; Lee, S. S.; Park, J.; Chung, Y.; Na, H. B. *J. Am. Chem. Soc.* **2001**, *123*, 12798.
47. Luna-Martínez, J. F.; Reyes-Melo, E.; González-González, V.; Guerrero-Salazar, C.; Torres-Castro, A.; Sepúlveda-Guzmán, S. *J. Appl. Polym. Sci.* **2013**, *127*, 2325.
48. Caraschi, J. C.; Leão, A. L. *Mol. Cryst. Liq. Cryst. Sci. Technol. Sect. Mol. Cryst. Liq. Cryst.* **2000**, *353*, 149.
49. Li, R.; Fei, J.; Cai, Y.; Li, Y.; Feng, J.; Yao, J. *Carbohydr. Polym.* **2009**, *76*, 94.
50. O'Connor, D.; Blum, F. D. *J. Appl. Polym. Sci.* **1987**, *33*, 1933.